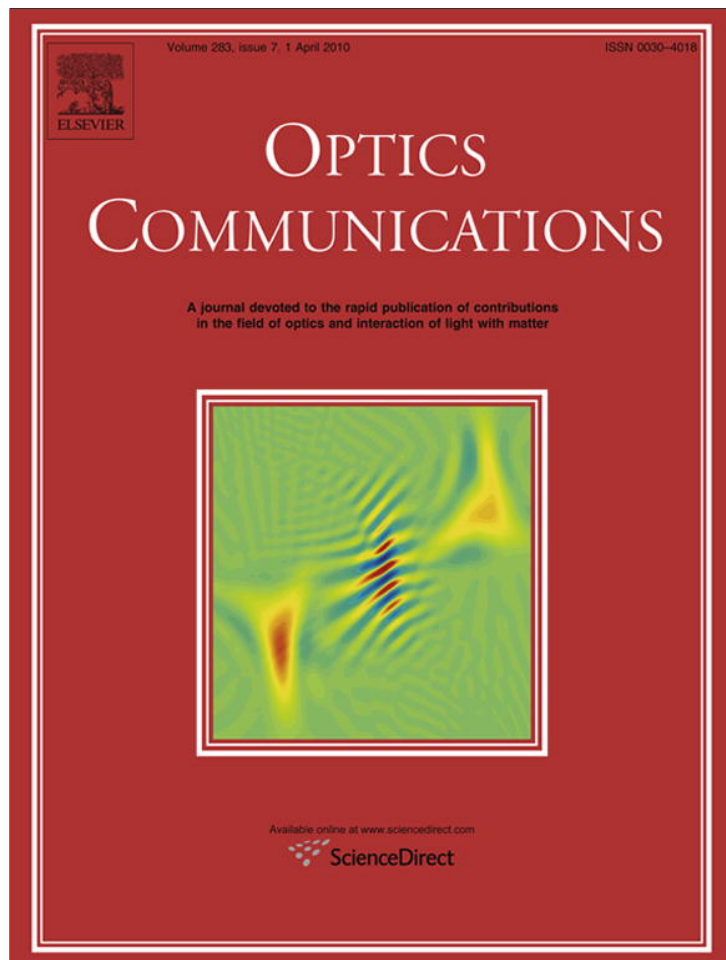


Provided for non-commercial research and education use.  
Not for reproduction, distribution or commercial use.



This article appeared in a journal published by Elsevier. The attached copy is furnished to the author for internal non-commercial research and education use, including for instruction at the authors institution and sharing with colleagues.

Other uses, including reproduction and distribution, or selling or licensing copies, or posting to personal, institutional or third party websites are prohibited.

In most cases authors are permitted to post their version of the article (e.g. in Word or Tex form) to their personal website or institutional repository. Authors requiring further information regarding Elsevier's archiving and manuscript policies are encouraged to visit:

<http://www.elsevier.com/copyright>



Contents lists available at ScienceDirect

Optics Communications

journal homepage: [www.elsevier.com/locate/optcom](http://www.elsevier.com/locate/optcom)

# Measurement of atmospheric turbulence strength by vortex beam

Yalong Gu\*, Greg Gbur

Department of Physics and Optical Science, University of North Carolina at Charlotte, Charlotte, NC 28223, United States

## ARTICLE INFO

### Article history:

Received 22 September 2009

Received in revised form 18 November 2009

Accepted 19 November 2009

## ABSTRACT

The behavior of spatial correlation singularities suggests a possible method for measuring atmospheric turbulence strength with a vortex beam. The refractive index structure constant  $C_n^2$  can be obtained by measuring the radius of a ring dislocation of a vortex beam which has passed through atmospheric turbulence. An approximate analytic expression for the radius of a ring dislocation as a function of  $C_n^2$  has been derived, and its accuracy is verified by numerical examples.

© 2009 Elsevier B.V. All rights reserved.

## 1. Introduction

The effects of atmospheric turbulence on the propagation of optical beams, such as scintillation, beam wander, decrease of coherence, and beam spreading, have been actively researched for many years [1–3]. These effects arise from the turbulence-induced random phase modulation of the optical field. As a result, the performance of a long-range optical system operating in the atmosphere strongly depends upon the turbulence characteristics.

In particular, the refractive index structure constant  $C_n^2$ , which characterizes the turbulence strength, also dictates the strength of scintillations. Scintillation is the primary limitation in the development of free-space optical communication systems. Techniques for minimizing scintillation, such as using partially coherent beams (see, for instance, [4,5]), requires knowledge of the value of  $C_n^2$ , which must be measured independently for an optimal solution.

The traditional method to measure  $C_n^2$  is to use an optical scintillometer [6–8]. By measuring the scintillation of a wavefield over a short propagation distance, the path-averaged value of  $C_n^2$  is obtained. A recent study on the behavior of spatial correlation singularities, however, suggests an alternate solution. Spatial correlation singularities, also referred to as coherence vortices [9], are the zeros of the cross-spectral density function at which the phase is undefined. A ring dislocation has been shown to exist in the cross-correlation function of a partially coherent field when passed through a vortex mask [10,11]. In recent studies, the properties of the ring dislocation in the presence of fluctuations and on propagation in free space were investigated [12,13]. It is demonstrated that the radius of this ring dislocation is inversely related to coherence length of the wavefield. As spatial coherence decreases on propagation through turbulence, it is reasonable to ask whether a mea-

surement of such a ring dislocation could be used as a measure of turbulence strength, namely  $C_n^2$ .

In this paper, we show that it is feasible to measure turbulence strength by vortex beam propagation. An approximate analytic expression of the radius of a ring dislocation as a function of  $C_n^2$  has been derived. The condition for the accuracy of approximation is given through numerical examples.

## 2. Theory

The propagation geometry is illustrated in Fig. 1. The vortex beam is generated by passing a Gaussian beam through an idealized vortex mask at the transmitter plane. By using the extended Huygens–Fresnel principle [14], the transmitted field at the receiver plane  $z = L$  (in the far-field regime) can be expressed in the form

$$U(\rho, L) = -\frac{ik}{2\pi L} \exp\left(ikL + \frac{ik\rho^2}{2L}\right) \times \int U(\rho', 0) \times \exp\left[-i2\pi \frac{\rho}{\lambda L} \cdot \rho' + \psi(\rho, \rho')\right] d^2\rho', \quad (1)$$

where  $U(\rho', 0) = \exp(-\rho'^2/w_0^2) \exp(i\phi')$  is the field at the transmitter plane,  $k$  is the wavenumber,  $w_0$  is the beam width at the transmitter plane, and  $\psi(\rho, \rho')$  is the random part of the complex phase of a spherical wave propagating in turbulence. Coherence properties of the field at the receiver plane are characterized by the cross-spectral density [15]

$$\begin{aligned} W(\rho_1, \rho_2, L) &= \langle U^*(\rho_1, L)U(\rho_2, L) \rangle \\ &= A \iint U^*(\rho'_1, 0)U(\rho'_2, 0) \\ &\quad \times \exp\left[i2\pi \left(\frac{\rho_1 \cdot \rho'_1 - \rho_2 \cdot \rho'_2}{\lambda L}\right)\right] \\ &\quad \times \langle \exp[\psi^*(\rho_1, \rho'_1) + \psi(\rho_2, \rho'_2)] \rangle d^2\rho'_1 d^2\rho'_2, \quad (2) \end{aligned}$$

\* Corresponding author.

E-mail address: [ygu4@uncc.edu](mailto:ygu4@uncc.edu) (Y. Gu).

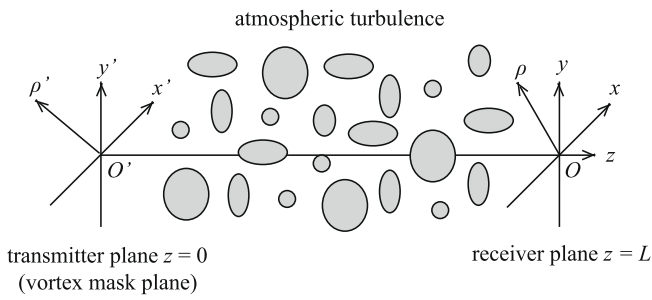


**Fig. 1.** Illustration of the propagation geometry. The vortex mask of order 1 is placed at the transmitter plane  $z = 0$ . It imparts a phase factor  $\exp(i\psi')$  to the incident Gaussian beam  $U_0 = \exp(-\rho^2/w_0^2)$ . For simplicity, the waist plane of the Gaussian beam is also at the transmitter plane.

where  $A = (1/\lambda L)^2 \exp[ik(\rho_2^2 - \rho_1^2)/(2L)]$ , the asterisk indicates complex conjugate, and the angular brackets denote an ensemble average over the turbulence fluctuations. When turbulence is homogeneous, the random part of the complex phase of a spherical wave in Eq. (2) can be approximated by [16]

$$\langle \exp [\psi^*(\rho_1, \rho'_1) + \psi(\rho_2, \rho'_2)] \rangle \approx \exp \left( -\frac{|\mathbf{r}|^2 + \mathbf{r} \cdot \mathbf{r}' + |\mathbf{r}'|^2}{\rho_0^2} \right) = T(\mathbf{r}', \mathbf{r}), \quad (3)$$

where

$$\rho_0 = (0.55 C_n^2 k^2 L)^{-3/5} \quad (4)$$

is the coherence length of a spherical wave propagating in turbulence,  $\mathbf{r} = \rho_2 - \rho_1$ ,  $\mathbf{r}' = \rho'_2 - \rho'_1$ , and  $C_n^2$  is the refractive index structure constant. In this paper, we assume that  $C_n^2$  is a constant over the propagation path. In the Appendix, we show that it can also represent the average value if  $C_n^2$  is varying on propagation. Although the quadratic approximation of the random phase structure function in Eq. (3) has certain limits [17], it gives a good approximation of the second order statistical properties of fields in turbulence under many circumstances. With this approximation, the cross-spectral density at the receiver plane can be written as

$$W(\rho_1, \rho_2, L) = A \iint U^*(\rho'_1, 0) U(\rho'_2, 0) T(\mathbf{r}', \mathbf{r}) \times \exp \left[ i2\pi \left( \frac{\rho_1 \cdot \rho'_1 - \rho_2 \cdot \rho'_2}{\lambda L} \right) \right] d^2 \rho'_1 d^2 \rho'_2. \quad (5)$$

Eq. (5) may be expressed in a more suggestive form by using the following Fourier expansions,

$$T(\mathbf{r}', \mathbf{r}) = \int \tilde{T}(\boldsymbol{\kappa}, \mathbf{r}) \exp(i2\pi \mathbf{r}' \cdot \boldsymbol{\kappa}) d^2 \boldsymbol{\kappa}, \quad (6)$$

$$U(\rho'_j, 0) = \int \tilde{U}(\boldsymbol{\kappa}_j, 0) \exp(i2\pi \rho'_j \cdot \boldsymbol{\kappa}_j) d^2 \boldsymbol{\kappa}_j \quad (j = 1, 2). \quad (7)$$

On substituting Eqs. (6) and (7) into Eq. (5) and applying standard Fourier transform techniques, one can find that

$$W(\rho_1, \rho_2, L) = A \int \tilde{U}^* \left( \frac{\rho_1}{\lambda L} - \boldsymbol{\kappa}, 0 \right) \tilde{U} \left( \frac{\rho_2}{\lambda L} - \boldsymbol{\kappa}, 0 \right) \tilde{T}(\boldsymbol{\kappa}, \mathbf{r}) d^2 \boldsymbol{\kappa}, \quad (8)$$

where

$$\tilde{T}(\boldsymbol{\kappa}, \mathbf{r}) = \pi \rho_0^2 \exp(-\pi^2 \rho_0^2 \boldsymbol{\kappa}^2) \exp \left( -\frac{3|\mathbf{r}|^2}{4\rho_0^2} + i\pi \mathbf{r} \cdot \boldsymbol{\kappa} \right), \quad (9)$$

$$\tilde{U}(\boldsymbol{\kappa}, 0) = -\frac{i}{2} \pi^{5/2} w_0^3 \boldsymbol{\kappa} \exp(i\theta) \exp \left( -\frac{1}{2} \pi^2 w_0^2 \boldsymbol{\kappa}^2 \right) \times \left[ I_0 \left( \frac{1}{2} \pi^2 w_0^2 \boldsymbol{\kappa}^2 \right) - I_1 \left( \frac{1}{2} \pi^2 w_0^2 \boldsymbol{\kappa}^2 \right) \right]. \quad (10)$$

In Eq. (10),  $\theta$  is the azimuthal angle of  $\boldsymbol{\kappa}$ ,  $I_0$  and  $I_1$  are the zero and first order modified Bessel function of the first kind respectively. With Eqs. (9) and (10), Eq. (8) can be written as

$$W(\rho_1, \rho_2, L) = A \exp \left( -\frac{3|\mathbf{r}|^2}{4\rho_0^2} \right) \int U_1^*(\rho_1, \boldsymbol{\kappa}) U_1(\rho_2, \boldsymbol{\kappa}) p(\boldsymbol{\kappa}) d^2 \boldsymbol{\kappa}, \quad (11)$$

where

$$p(\boldsymbol{\kappa}) = \pi \rho_0^2 \exp(-\pi^2 \rho_0^2 \boldsymbol{\kappa}^2), \quad (12)$$

$$U_1(\rho_j, \boldsymbol{\kappa}) = \tilde{U} \left( \frac{\rho_j}{\lambda L} - \boldsymbol{\kappa}, 0 \right) \exp(i\pi \boldsymbol{\kappa} \cdot \boldsymbol{\rho}_j) \quad (j = 1, 2). \quad (13)$$

The direct evaluation of Eq. (11) by substituting Eqs. (10), (12), and (13) is difficult. However, it can be simplified by using the following approximation for  $\tilde{U}(\boldsymbol{\kappa}, 0)$

$$\tilde{U}(\boldsymbol{\kappa}, 0) \approx -\frac{i}{2} \pi^{5/2} w_0^3 \boldsymbol{\kappa} \exp(i\theta) \exp \left( -\frac{1}{2} \pi^2 w_0^2 \boldsymbol{\kappa}^2 \right). \quad (14)$$

This expression contains only the lowest nonzero term of the series expansion of the modified Bessel functions in Eq. (10). With Eqs. (12) and (13), one can show that the cross-spectral density at the receiver plane (Eq. (11)) can be explained by the ‘beam wander’ model [18]. The field  $U_1$  is centered on a transverse location  $\boldsymbol{\kappa}$ .  $p(\boldsymbol{\kappa})$ , which satisfies  $\int p(\boldsymbol{\kappa}) d^2 \boldsymbol{\kappa} = 1$ , is the probability distribution function of  $\boldsymbol{\kappa}$  which limits the circular area where the field center can wander. The radius of this area is inversely related to  $\rho_0$ . For a large  $\rho_0$ , the field only wanders in a small area around the origin. Considering the fact that the difference between Eqs. (10) and (14) is negligible when the argument is small, the evaluation of Eq. (11) is accurate for small  $|\rho_1|$  and  $|\rho_2|$  by substituting Eqs. (12)–(14). On substitution and choosing  $(\rho_1, \rho_2)$  to be  $(\rho, -\rho)$ , the approximate cross-spectral density at the receiver plane is

$$W(\rho, -\rho, L) = \frac{\pi^6 w_0^6 \rho_0^2}{4\lambda^2 L^2} \exp \left\{ -\left[ \frac{\pi^2 w_0^2}{\lambda^2 L^2} + \frac{3}{w_0^2 \sigma_c^2} + \frac{1}{w_0^2 (1 + \sigma_c^2)} \right] \rho^2 \right\} \times \left[ \frac{1}{\pi^3 w_0^4 (1 + \sigma_c^2)^2} - \frac{\lambda^2 L^2 + \pi^2 w_0^4 (1 + \sigma_c^2)^2}{\pi^3 \lambda^2 L^2 w_0^6 (1 + \sigma_c^2)^3} \rho^2 \right], \quad (15)$$

where

$$\sigma_c = \rho_0/w_0 \quad (16)$$

is the relative coherence length which is a measure of the global spatial coherence of a beam on propagation through turbulence. From Eq. (15), it shows that there exist spatial correlation singularities at which the amplitude of the cross-spectral density  $W(\rho, -\rho)$  is zero and the phase is undefined. These spatial correlation singularities form a ring dislocation whose radius is

$$\rho = \lambda L \left[ \frac{w_0^2 (1 + \sigma_c^2)}{\lambda^2 L^2 + \pi^2 w_0^4 (1 + \sigma_c^2)^2} \right]^{1/2}. \quad (17)$$

### 3. Examples and analysis

Eq. (17) is the central analytic result of this paper. Fig. 2 shows the radius of a ring dislocation as a function of the turbulence strength parameter  $C_n^2$ . It can be seen that the radius of the dislocation increases monotonically with a considerable dynamic range in weak and moderate turbulence, eventually saturating for exceedingly strong turbulence. The simulated radii of some different  $C_n^2$  obtained by propagating a Gaussian beam through a vortex mask and turbulence are also shown in Fig. 2. We applied a multiple phase screen method for the simulations [19]. They have good agreement with the radii calculated from Eq. (17).

As the radius of a ring dislocation can be measured by a wave-front folding interferometer [10], Eq. (17) suggests that  $C_n^2$  can be

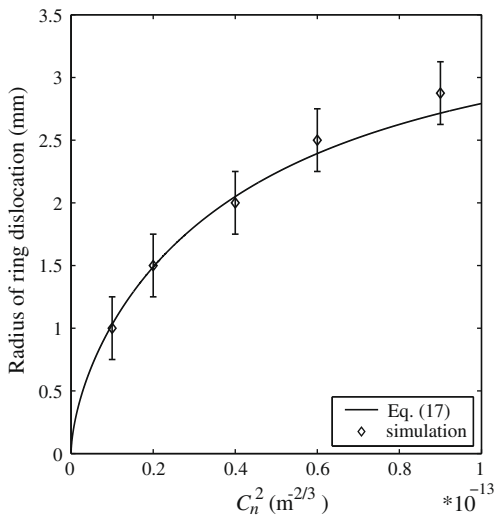


**Fig. 2.** Illustration of the radius of a ring dislocation as a function of  $C_n^2$ . The solid curve represents analytic result calculated from Eq. (17), while the unfilled shapes  $\diamond$  represent numerical result. The error bars represent the spatial resolution of the simulations. The propagation distance is taken to be  $L = 300$  m,  $\lambda = 1.55$   $\mu\text{m}$ , and the beam width  $w_0 = 4$  cm.

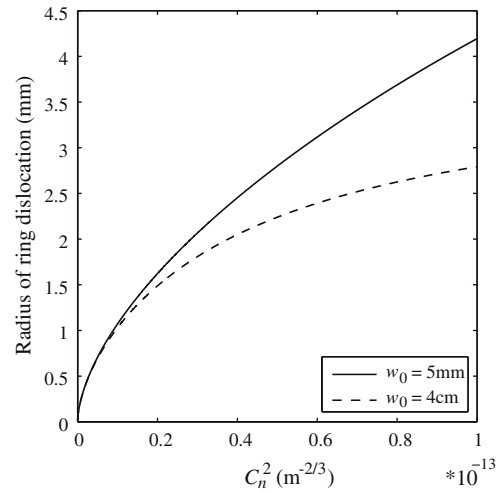


**Fig. 4.** Illustration of the radius of a ring dislocation of different beam width  $w_0$ . The curves are calculated from Eq. (17). The propagation distance is taken to be  $L = 300$  m and  $\lambda = 1.55$   $\mu\text{m}$ .

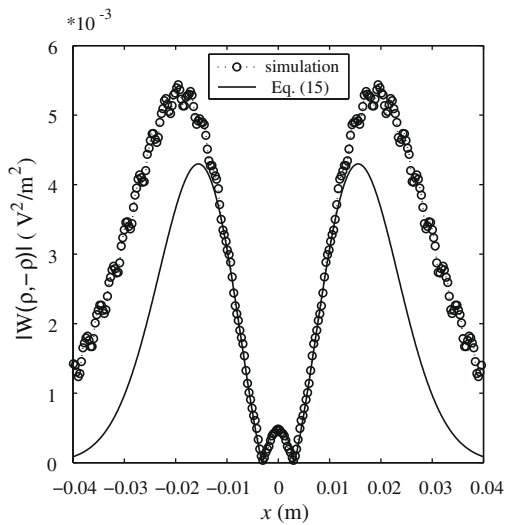


**Fig. 3.** The transverse distribution of the absolute value of the cross-spectral density  $W(\rho, -\rho)$  at the receiver plane ( $L = 250$  m). The solid curve represents analytic result calculated from Eq. (15), while the unfilled shapes  $\circ$  represent numerical result. The wavelength is taken to be  $\lambda = 1.55$   $\mu\text{m}$ ,  $C_n^2 = 10^{-13}$   $\text{m}^{-2/3}$ , and the beam width is taken to be  $w_0 = 5$  mm.

obtained by measuring the radius of such a ring dislocation at the receiver plane. However, it is necessary to give the condition for its accuracy. An example of the absolute value of the cross-spectral density  $W(\rho, -\rho)$  calculated from Eq. (15) is shown in Fig. 3. As a comparison, the numerical result obtained by simulation is also shown in Fig. 3. The relative coherence length  $\sigma_c$  is 7.73, which indicates high spatial coherence. As shown by Fig. 3, the numerical result of  $|W(\rho, -\rho)|$  and the analytic result calculated from Eq. (15) have good agreement in the central area around the origin. The simulated radius of such a ring dislocation is 3 mm, while the radius calculated from Eq. (17) is 3.2 mm. Therefore, the approximate analytic expression of the radius of a ring dislocation Eq. (17) is accurate for large relative coherence length  $\sigma_c$ . By numerical simulation, we have found that Eq. (17) is accurate when  $\sigma_c > 0.9$ .

It is worth noting that  $C_n^2$  can be obtained by measuring the radius of a ring dislocation even in the strong turbulence regime. As illustrated by Fig. 3, it can be anticipated that the variation of the radius of a ring dislocation is small in the strong turbulence regime. Therefore  $C_n^2$  may be undistinguishable due to the limited resolution of an image system. However, considering the fact that saturation in the strong turbulence regime corresponds to low spatial coherence at the receiver plane, it can be solved by increasing spatial coherence, namely increasing the relative coherence length  $\sigma_c$  by decreasing either the beam width  $w_0$  or the propagation distance  $L$ . As shown in Fig. 4, for a Gaussian beam with a small beam width, the radius of the ring dislocation still has a certain dynamic range even in the strong turbulence regime.

**4. Conclusions**

In this paper, we theoretically investigated the feasibility of atmospheric turbulence strength measurement by vortex beam propagation. It is demonstrated that, by appropriately choosing beam and propagation parameters, the atmospheric turbulence strength parameter  $C_n^2$  or its averaged value when  $C_n^2$  is varying on propagation can be obtained by measuring the radius of a ring dislocation after a vortex beam passes through turbulence, even in the saturated regime.

Although the proposed method in this paper is focused on the measurement of atmospheric turbulence strength, in principle it can be extended to the measurement of other weakly scattering random media or random fields. For example, it can be used to measure the statistical parameters of tissue [20] or the coherence length of a Gaussian Schell-model beam. In general, it suggests a relatively straightforward and flexible method to study the statistical properties of a random medium or a random field.

**Acknowledgements**

This research was supported by the Air Force Office of Scientific Research under Grant FA9550-08-1-0063.

**Appendix A**

In this appendix, we show that when the refractive index structure constant  $C_n^2$  is varying on the propagation, the average value

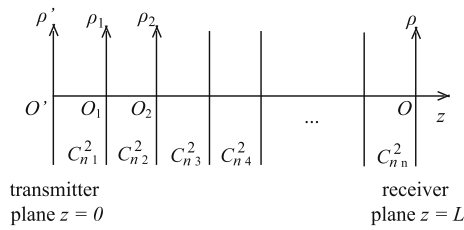


**Fig. 5.** Illustration of the propagation geometry in the case of varying  $C_n^2$ . The whole propagation path is divided into  $n$  slabs. The thickness of each slab is  $L/n$ .  $C_n^2$  is the refractive index structure constant in the  $i$ th slab, while  $i = 1, 2, \dots, n$ .

$\overline{C_n^2}$  can still be obtained by measuring the radius of a ring dislocation at the receiver plane.

As illustrated by Fig. 5, atmospheric turbulence between the transmitter plane and the receiver plane can be divided into slabs of equal thickness. By the slow-varying assumption,  $C_n^2$  in each slab is a constant and the difference of  $C_n^2$  in each two adjacent slabs is small. We take the propagation in the first two slabs as an example. By the extended Huygens–Fresnel principle and the quadratic approximation of the random phase structure function, the cross-spectral densities at the plane  $z = L/n$  and  $z = 2L/n$  are

$$W_2(\mathbf{R}_2, \mathbf{r}_2) \propto \int d^2R' \int d^2r' W_0(\mathbf{R}', \mathbf{r}') \times \exp\left(-\frac{|\mathbf{r}_2|^2 + \mathbf{r}_2 \cdot \mathbf{r}' + |\mathbf{r}'|^2}{\overline{\rho}_{12}^2}\right) \times \exp\left[\frac{ink}{2L}(\mathbf{R}' \cdot \mathbf{r}' + \mathbf{R}_2 \cdot \mathbf{r}_2 - \mathbf{R}' \cdot \mathbf{r}_2 - \mathbf{R}_2 \cdot \mathbf{r}').\right] \quad (A6)$$

By comparing Eqs. (A5) and (A6), one can find that

$$\overline{\rho_{12}^2} = \frac{1}{\sqrt{2}} \rho_{01} \rho_{02}. \quad (A7)$$

When the field is propagating into the third slab, the first two slab can be treated as a unity whose average coherence length of a spherical wave is  $\overline{\rho}_{12}$ . By the similar derivation, one can show that the average coherence length of a spherical wave in the whole propagation path  $L$  is

$$\overline{\rho_0^2} = 2^{-\frac{1}{2}-2(\frac{1}{2})^n} \rho_{01}^{\frac{1}{2^{n-2}}} \rho_{02}^{\frac{1}{2^{n-2}}} \prod_{i=3}^n \rho_{0i}^{\frac{1}{2^{n-i}}} \quad (n \geq 3), \quad (A8)$$

$$W_1(\rho_{11}, \rho_{12}) \propto \iint W_0(\rho'_1, \rho'_2) \exp\left[-\frac{ink}{2L}(|\rho_{11} - \rho'_1|^2 - |\rho_{12} - \rho'_2|^2)\right] \times \exp\left(-\frac{|\mathbf{r}_1|^2 + \mathbf{r}_1 \cdot \mathbf{r}' + |\mathbf{r}'|^2}{\rho_{01}^2}\right) d^2\rho'_1 d^2\rho'_2, \quad (A1)$$

$$W_2(\rho_{21}, \rho_{22}) \propto \iint W_1(\rho_{11}, \rho_{12}) \exp\left[-\frac{ink}{2L}(|\rho_{21} - \rho_{11}|^2 - |\rho_{22} - \rho_{12}|^2)\right] \times \exp\left(-\frac{|\mathbf{r}_2|^2 + \mathbf{r}_2 \cdot \mathbf{r}_1 + |\mathbf{r}_1|^2}{\rho_{02}^2}\right) d^2\rho_{11} d^2\rho_{12}, \quad (A2)$$

where  $W_0(\rho'_1, \rho'_2)$  is the cross-spectral density at the transmitter plane,  $\rho_{01} = (0.55C_{n1}^2 k^2 L/n)^{-3/5}$ ,  $\rho_{02} = (0.55C_{n2}^2 k^2 L/n)^{-3/5}$ ,  $\mathbf{r}' = \rho'_2 - \rho'_1$ ,  $\mathbf{r}_1 = \rho_{12} - \rho_{11}$  and  $\mathbf{r}_2 = \rho_{22} - \rho_{21}$ . For convenience, we introduce the new variables  $(\mathbf{R}', \mathbf{r}')$ ,  $(\mathbf{R}_1, \mathbf{r}_1)$  and  $(\mathbf{R}_2, \mathbf{r}_2)$ , where  $\mathbf{R}' = (\rho'_2 + \rho'_1)/2$ ,  $\mathbf{R}_1 = (\rho_{12} + \rho_{11})/2$  and  $\mathbf{R}_2 = (\rho_{22} + \rho_{21})/2$ . On substituting Eq. (A1) into Eq. (A2) and taking integral with respect to  $(\mathbf{R}_1, \mathbf{r}_1)$ , the cross-spectral density at plane  $z = 2L/n$  can be written as

$$W_2(\mathbf{R}_2, \mathbf{r}_2) \propto \int d^2R' \int d^2r' W_0(\mathbf{R}', \mathbf{r}') \times \exp\left[-\frac{(\rho_{02}^2 + 7\rho_{01}^2)|\mathbf{r}_2|^2 + 4(\rho_{01}^2 + \rho_{02}^2)\mathbf{r}_2 \cdot \mathbf{r}' + (7\rho_{01}^2 + \rho_{02}^2)|\mathbf{r}'|^2}{4\rho_{01}^2 \rho_{02}^2}\right] \times \exp\left[\frac{ink}{2L}(\mathbf{R}' \cdot \mathbf{r}' + \mathbf{R}_2 \cdot \mathbf{r}_2 - \mathbf{R}' \cdot \mathbf{r}_2 - \mathbf{R}_2 \cdot \mathbf{r}').\right] \quad (A3)$$

By the assumption of small difference of  $C_n^2$  in the two adjacent slabs, we can assume that

$$\rho_{02}^2 + 7\rho_{01}^2 \approx 4(\rho_{01}^2 + \rho_{02}^2) \approx 7\rho_{01}^2 + \rho_{02}^2 \approx 8\overline{\rho_{12}^2}, \quad (A4)$$

where  $\overline{\rho_{12}}$  is the average coherence length of a spherical wave in the first two slabs. On substituting Eq. (A4), Eq. (A3) can be written as

$$W_2(\mathbf{R}_2, \mathbf{r}_2) \propto \int d^2R' \int d^2r' W_0(\mathbf{R}', \mathbf{r}') \times \exp\left[-\frac{2\overline{\rho_{12}^2}(|\mathbf{r}_2|^2 + \mathbf{r}_2 \cdot \mathbf{r}' + |\mathbf{r}'|^2)}{\rho_{01}^2 \rho_{02}^2}\right] \times \exp\left[\frac{ink}{2L}(\mathbf{R}' \cdot \mathbf{r}' + \mathbf{R}_2 \cdot \mathbf{r}_2 - \mathbf{R}' \cdot \mathbf{r}_2 - \mathbf{R}_2 \cdot \mathbf{r}').\right] \quad (A5)$$

$W_2(\mathbf{R}_2, \mathbf{r}_2)$  can also be calculated from  $W_0(\mathbf{R}', \mathbf{r}')$  by the extended Huygens–Fresnel principle directly, which is

where

$$\overline{\rho_0} = (0.55\overline{C_n^2} k^2 L)^{-3/5} \quad (A9)$$

$$\rho_{0i} = (0.55C_{ni}^2 k^2 L/n)^{-3/5} \quad (i = 1, 2, \dots, n).$$

We can readily see that the average value  $\overline{C_n^2}$  can be measured by the radius of a ring dislocation when it is varying along the propagation path, while  $C_n^2$  is defined by Eqs. (A8) and (A9).

### References

- [1] A. Ishimaru, Wave Propagation and Scattering in Random Media, Academic Press, San Diego, CA, 1978.
- [2] R.L. Fante, Wave propagation in random media: a systems approach, in: E. Wolf (Ed.), Progress in Optics, vol. 22, Elsevier, Amsterdam, 1985, p. 341.
- [3] L.C. Andrews, R.L. Phillips, Laser Beam Propagation through Random Media, SPIE Press, Bellingham, WA, 1998.
- [4] J.C. Leader, J. Opt. Soc. Am. 69 (1979) 73.
- [5] V.A. Banakh, V.M. Buldakov, V.L. Mironov, Opt. Spectrosc. 54 (1983) 1054.
- [6] A.V. Artem'ev, A.S. Gurvich, Radiophys. Quantum Electron. 14 (1971) 580.
- [7] T. Wang, G.R. Ochs, S.F. Clifford, J. Opt. Soc. Am. 68 (1978) 334.
- [8] R.J. Hill, G.R. Ochs, J. Opt. Soc. Am. A 9 (1992) 1406.
- [9] G. Gbur, T.D. Visser, Opt. Commun. 222 (2003) 117.
- [10] D.M. Palacios, I.D. Maleev, A.S. Marathay, G.A. Swartzlander Jr., Phys. Rev. Lett. 92 (2004) 143905.
- [11] I.D. Maleev, D.M. Palacios, A.S. Marathay, G.A. Swartzlander Jr., J. Opt. Soc. Am. B 21 (2004) 1895.
- [12] G.A. Swartzlander Jr., R.I. Hernandez-Aranda, Phys. Rev. Lett. 99 (2007) 169301.
- [13] I.D. Maleev, G.A. Swartzlander Jr., J. Opt. Soc. Am. B 25 (2008) 915.
- [14] R.F. Lutomirski, H.T. Yura, Appl. Opt. 10 (1971) 1652.
- [15] L. Mandel, E. Wolf, Optical Coherence and Quantum Optics, Cambridge University Press, Cambridge, UK, 1995.
- [16] H.T. Yura, Appl. Opt. 11 (1972) 1399.
- [17] S.M. Wandzura, J. Opt. Soc. Am. 70 (1980) 745.
- [18] G. Gbur, T.D. Visser, E. Wolf, Pure Appl. Opt. 6 (2004) S239.
- [19] J.M. Martin, S.M. Flatté, Appl. Opt. 27 (1988) 2111.
- [20] W. Gao, O. Korotkova, Opt. Commun. 270 (2007) 474.